RESEARCH DEPARTMENT REPORT SERIES no. 69-2010 ISSN 1749-8775

GROUNDWELL RIDGE, SWINDON
ARCHAEOMAGNETIC DATING REPORT, JULY 2005

Paul Linford

ARCHAEOLOGICAL SCIENCE

ENGLISH HERITAGE

GROUNDWELL RIDGE, SWINDON

ARCHAEOMAGNETIC DATING REPORT, JULY 2005

Paul Linford

NGR: SU 141 894

ISSN 1749-8775

SUMMARY

Two stone-lined Roman flue features from an English Heritage excavation in 2005 at Groundwell Ridge in Swindon were sampled for archaeomagnetic dating. The first (1GW, context 10062) appeared to have been well fired during the Roman period but analysis of a strong viscous remanence component suggested it had subsequently been disturbed. Enough undisturbed material was identified to date the last firing of the feature to between AD 170 and AD 305 using the 1988 UK calibration curve of Clark, Tarling and Noel. This date range is, however, of poorer precision than might be expected for a Roman feature that had not been subject to disturbance. The second feature (2GW, 10060) proved not to have been exposed to sufficient heat for a stable thermoremanent magnetisation to form and could not be dated using archaeomagnetism. A summary of key information for archaeomagnetic database compilers can be found on page 8.

CONTRIBUTORS

Fieldwork was carried out by Louise Martin and Paul Linford, subsequent laboratory analyses and reporting were carried out by Paul Linford.

ACKNOWLEDGEMENTS

The author is grateful to Dr Peter Wilson of English Heritage for bringing the feature to his attention and inviting the Geophysics Team to sample it.

ARCHIVE LOCATION

Fort Cumberland

DATE OF FIELDWORK AND REPORT

The fieldwork was conducted on 22nd July 2005 and the report was completed on the 30th July 2010.

CONTACT DETAILS

Geophysics Team, English Heritage, Fort Cumberland, Fort Cumberland Road, Eastney, Portsmouth PO4 9LD.
Paul Linford; Tel: 023 9285 6749; Email: paul.linford@english-heritage.org.uk

CONTENTS

INTRODUCTION

During development of land at Groundwell Ridge to the north of Swindon for housing in the mid 1990s remains of substantial Roman walls were unearthed which further archaeological investigations revealed to be part of an extensive villa or ceremonial complex (Corney 1997 ; Phillips and Walters 1997). The site was also the focus for an extensive programme of geophysical survey by the English Heritage (EH) Geophysics Team (Linford 1999 ; Linford 2002 ; Linford and Martin 2002 ; Linford and Linford 2004) and in 2005 the English Heritage Centre for Archaeology conducted more extensive excavations of the buried remains of the more substantial structures that had been detected.

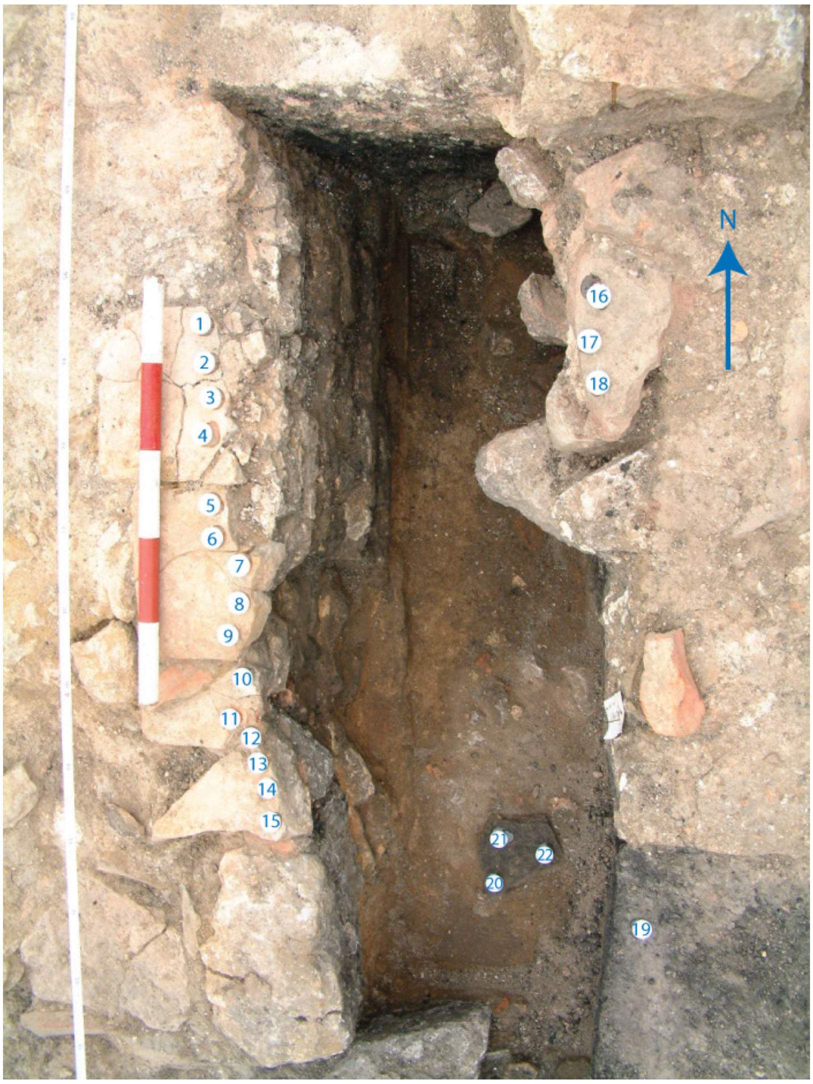

Figure 1: Photograph of feature 1GW (context 10062) showing the locations of the numbered archaeomagnetic sampling discs. The scale rule positioned on the left is 0.5 m long.

During these excavations two flue structures thought to be associated with a heating system for a Roman bath house were uncovered (see Figures 1 and 2) and, given that both exhibited visual evidence suggesting they had been exposed to high temperatures during operation, Dr Peter Wilson, who directed the excavation, requested that they be sampled for archaeomagnetic dating. The site, located at Ordnance Survey National Grid Reference SU 141 894, longitude 1.8° W and latitude 51.6 ° N, was visited for this purpose on the 22nd July 2005. Louise Martin of the EH Geophysics Team assisted with the sampling, and all subsequent measurement and analysis was carried out by the author.

Figure 2: Photograph of feature 2GW (context 10060) showing the locations of the numbered archaeomagnetic sampling discs. The long scale rule positioned slightly right of centre is 0.5 m long.

METHOD

Specimens were collected from both features using the disc method (see appendix, section 1a) and orientated to true north using a gyro-theodolite. The archaeomagnetic feature prefix codes 1GW and 2GW were given to specimens taken from contexts 10062 and 10060 respectively. The majority of the specimens were taken from blocks of the local Corallian Limestone of which the two features were primarily composed, although some specimens from feature 2GW (as indicated in Table 10) were of fired soil containing Oxford Clay. The distribution of specimen discs around the two features is shown in Figures 1 and 2. Twenty-two specimens were recovered from feature 1GW and twelve from feature 2GW. Stone specimens were cut to an appropriate size for measurement in the laboratory using a stone cutting disc, while fired clay specimens were consolidated using a Vinamul 40224 solution.

During preparation, the orientation discs of specimens 1GW10, 1GW19 and 1GW20 became detached and these specimens were therefore abandoned. The epoxy resin used for the Groundwell sampling was found to be inexplicably friable and the discs attached to specimens 1GW01, 1GW05, 1GW07, 1GW08, 1GW09, 1GW15 and 1GW21 became detached during measurement. In most cases it was possible to re-affix them and continue as the necessary directional information was marked directly onto the material of each specimen as a precaution once this problem became apparent. However, for the first two such specimens, 1GW09 and 1GW15, the precautionary markings had not been made. For 1GW09 a correction for subsequent measurements was made by assuming that that the declination angle of the magnetisation remained constant between the 5 and 7.5 mT demagnetisation stages (not unreasonable as the declination angle had varied through only ~0.5° during the preceding low coercivity demagnetisations). However, further demagnetisation was abandoned on 1GW15 after the disc became detached at the 20 mT stage where such an assumption would not have been justifiable.

The natural remanent magnetisation (NRM) measured in archaeomagnetic specimens is assumed to be caused by thermoremanent magnetisation (TRM) created at the time when the feature of which they were part was last fired. However, a secondary component acquired in later geomagnetic fields can also be present, caused by diagenesis or partial reheating. Additionally, the primary TRM may be overprinted by a viscous component, depending on the grain size distribution within the magnetic material. These secondary components are usually of lower stability than the primary TRM and can thus be removed by partial demagnetisation of the specimens.

To isolate these different components, each specimen is partially demagnetised. This involves tumbling the specimen in an alternating magnetic field of fixed peak strength and measuring the resulting changes in its magnetisation. This AF demagnetisation removes the contribution of the most weakly magnetised particles within the specimen (those with the lowest coercivities). The higher the peak field strength applied, the greater the proportion of the specimen's magnetisation that is removed. The procedure is repeated with increasing peak field strengths to build up a complete picture of the coercivity spectrum (or demagnetisation curve) of the specimen.

NRM measurements were first made on all the Groundwell specimens, then all specimens from feature 1GW were demagnetised to 100mT using successive incremental demagnetising fields of 1, 2.5, 5, 7.5, 10, 15, 20, 30, 50, 75 and 100 mT (see Tables 2 to 8) although for 1GW15 demagnetisation was concluded after the 15 mT stage as already noted. The same incremental partial demagnetisation sequence was also applied to specimens 2GW08, 2GW09, 2GW11 and 2GW12 although demagnetisation of 2GW08 was concluded at the 50 mT stage as very little of the remanent field remained (Tables 11 and 12).

Principal components analysis can be used to determine the various linear segments present within the specimen's demagnetisation curve (Kirshvinck 1980). In the ideal case, each linear segment will correspond with one of the magnetisation components described above. Linearity is determined using the Maximum Angular Deviation (MAD) statistic (see Kirshvinck 1980 for definition). The smaller this statistic the better and, as a rule of thumb, sets of measurements with a MAD of <= 2.0° are considered acceptably linear. Once the linear segment corresponding to a specimen's primary magnetisation direction has been identified, its principal component is taken as the characteristic direction of remanent magnetisation (ChRM). The results of this analysis for the specimens from features 1GW and 2GW are listed in Tables 9 and 13 respectively where the range of demagnetisation increments for which each specimen showed the highest linearity is recorded along with the corresponding MAD angle and calculated mean direction of magnetisation.

Once the ChRM direction for each specimen from a feature has been determined, a mean ChRM direction can be calculated. Some specimens may be excluded from this calculation if their ChRM directions are so anomalous as to make them statistical outliers from the overall distribution. The mean direction is then adjusted according to the location of the feature relative to a notional central point in the UK (Meriden), so that it can be compared with standardised archaeomagnetic calibration data to produce a date of last firing for the feature.

Notes concerning the mean calculation and subsequent calibration can be found in sections 3 and 4 of the appendix. However, calibration of UK archaeomagnetic directions is in a period of transition at present. Until recently the UK archaeomagnetic calibration curve of Clark, Tarling and Noël (Clark *et al.* 1988) was routinely used to calibrate archaeomagnetic data from England as described in section 4 of the appendix. This curve was created before more recent computational and statistical developments allowed for an objective treatment of the uncertainty inherent in the calibration data itself to be taken into account when constructing the calibration curve. More recently a new curve has been created applying new Bayesian statistical methodologies and incorporating the wealth of new UK calibration material that has accumulated in the years since Clark *et al* published their curve (Zananiri *et al.* 2007). However, the curve of Clark *et al.* benefits from a great deal of qualitative refinement (via literature review and direct discussions with archaeologists) of the independent dating evidence associated with each magnetic direction in the calibration database used in its construction. It has not been possible, as yet, to undertake the same level of refinement on the much wider pool of data upon which the newer curve of Zananiri *et al.* is based. The latter curve currently tends to produce much broader date ranges than the former and, while some reduction in apparent precision is to be expected when using a calibration curve that objectively accounts for all the inherent sources of uncertainty, the precision of dates achieved using the Zananiri *et al.* curve is likely to become more consistent with that of existing archaeomagnetic dates once this refinement has been undertaken. Hence, while work proceeds to improve the independent dating evidence of the newer calibration evidence, the somewhat uneasy compromise must be adopted of quoting calibrations against both curves so that the date can both be compared with existing archaeomagnetic dates and remain compatible with future developments.

RESULTS

1GW (context number 10062)

Figure 3 compares the distribution of both specimen NRM directions and final ChRM directions established after partial demagnetisation and these are quite highly scattered with specimens 05, 06, 16-18, 21 and 22 being particularly anomalous. The measurements tabulated in Tables 1 to 8 indicate that the specimens were strongly magnetised suggesting that they were subjected to sufficient heat to form a thermoremanent magnetisation during the operation of the feature. A significant viscous remanent magnetisation component overprints the primary TRM at coercivities up to 10mT and this can be seen in the representative demagnetisation curves that have been plotted for specimens 01, 05, 14 and 22 (Figures 4-7 respectively), particularly in Figures 5 and 7 where the viscous component is in a markedly different direction to the primary TRM. However, the fact that the distribution of ChRM results after partial demagnetisation does not improve matters rules out viscous overprinting as the primary cause of the anomalous scattering of TRM directions. The only explanation remaining is that, despite appearing intact, the feature has been disturbed since it was last fired and the various constituent stone blocks are no longer in exactly the same orientation as they were at that time. Weight is lent to this conjecture by the observation that specimens taken from the same block (e.g. 05 and 06, 16-18, 21 and 22) exhibit very similar magnetisation directions even when these directions are highly anomalous.

The viscous remanent component persists to a high coercivity in most of the specimens, typically until the 10 mT demagnetisation step and in some cases up to 15 mT. This suggests that it has accumulated over a long period of time rather than being a short-term component acquired since the specimens were brought to the laboratory. The direction of the VRM component in each specimen was estimated by subtraction of its remaining magnetisation vector after 10 mT demagnetisation from that after 5 mT demagnetisation and the results are superimposed over the ChRM directions on Figure 3b in cyan. It is clear from comparison of the two sets of directions that the VRM directions are less scattered than the ChRM directions suggesting that the ChRM was acquired prior to the feature being disturbed while the VRM component has built up since the disturbance event. The conclusion to be drawn is, therefore, that the feature must have been disturbed in antiquity, possibly towards the end of the Roman period when the building housing it collapsed.

While most of the specimens appear to come from parts of the feature that have been subject to disturbance, it is clear from Table 9 that they all exhibit an acceptably stable and linear ChRM component. It was therefore decided to calculate a mean TRM direction and use the method of Beck (1983) to exclude the specimen ChRM directions most affected by disturbance by considering them as statistical outliers. The excluded specimens are indicated in the rightmost column of Table 1 and the mean TRM direction calculated from the twelve remaining is:

At site:	Dec = -3.98°	Inc = 58.08°	α_{95} = 4.67° k = 87.26 N=12
At Meriden:	Dec = -3.97°	Inc = 58.83°	

The disturbance to the feature and resulting scattering of the individual specimen remanence directions is reflected in the high alpha-95 value as a consequence of which any date range derived from this mean TRM determination will be of relatively low precision.

Calibration of the above archaeomagnetic direction with the two calibration curves cited above in the Method section is depicted in Figure 8 and results in the following date ranges:

Clark *et al*.: AD 170 to AD 305 at the 95% confidence level.
Zananiri *et al*.: AD 118 to AD 465 at the 95% confidence level.

In both cases a date range centred on the 14th century AD is also possible using purely archaeomagnetic considerations but it has been excluded as the site indubitably dates from the Roman period.

2GW (context number 10060)

Figure 9 depicts the distribution of specimen NRM directions from feature 2GW and it is immediately apparent that these are very highly scattered. The measurements tabulated in Table 9 indicate that the specimens have only a very weak magnetisation. The stone specimens (01-06) exhibit virtually no magnetisation whatsoever and it is likely that they were not subjected to sufficient heat for a thermoremanent magnetisation to be acquired.

To further investigate the slightly stronger magnetisation in the clay specimens (07-12) the four most strongly magnetised 08, 09, 11 and 12 were subjected to incremental partial demagnetisation and the results are depicted in Figures 10 to 14 respectively and tabulated in Tables 11 and 12. The measurements show that the primary magnetisation in the specimens is weak and that it is heavily overprinted by a viscous magnetisation component which, in the cases of 11 and 12, is in a direction almost directly opposed to the primary magnetisation. This suggests that the clay material was exposed to only relatively low temperatures not high enough for a stable remanent magnetisation to form. It is also likely that the clay has been disturbed since it was last exposed to heat accounting for the markedly different direction in which the subsequent viscous magnetisation has developed. Attempts to isolate a stable ChRM from the demagnetisation results (see Table 13) failed for 09 and have not improved the anomalous NRM directions in the cases of 11 and 12. It was thus concluded that 2GW could not be dated using archaeomagnetism.

CONCLUSIONS

Archaeomagnetic analysis of the remains of the two fired features from Groundwell has been only partially successful, providing a date for one of the two features sampled.

In the case of feature 1GW (context 10062), the measurements indicate it was initially subjected to a high degree of heating but that it has subsequently been disturbed. Given the strength of the viscous component that has accumulated in an entirely different direction to the primary magnetisation, it is likely the disturbance occurred in antiquity, perhaps when the building which housed the feature collapsed. It has, however, been possible to establish a date for the last firing of 1GW although at a lower precision than usual owing to the degree of disturbance. Taking the calibrations against the Clark *et al.* and Zananiri *et al.* curves together, it is most likely that the feature was last used in the 3rd century AD although there is a small chance that it continued in use into the 4th century (the most likely date range being that derived from the Clark *et al* curve, between AD 170 and AD 305).

Analysis of 2GW (context 10060) suggests that, despite its visual similarity to 1GW in both construction and colouration, the areas sampled were not subjected to a high enough temperature for a stable remanent magnetisation to form. It also exhibits some evidence of disturbance since it was last exposed to heat and these two facts together mean that it is unfortunately not possible to date it using archaeomagnetism.

ARCHAEOMAGNETIC DATE SUMMARY

Archaeomagnetic ID:	1GW	
Feature:	Roman flue feature, context 10062	
Location:	Longitude 1.8° W, Latitude 51.6° N	
Number of specimens (taken/used in mean):	22/12	
AF Demagnetisation Applied:	0-100mT (see text and Table 9)	
Distortion Correction Applied:	None	
Declination (at Meriden):	-3.98° (-3.97°)	
Inclination (at Meriden):	58.08° (58.83 °)	
Alpha-95:	4.67°	
k:	87.26	
Date range (95% confidence):	Clark *et al.*:	AD 170 to AD 305
	Zananiri *et al.*:	AD 118 to AD 465
Independent date estimate:	Roman	
Quality as calibration data:	Poor owing to disturbance post-firing	

Archaeomagnetic ID:	2GW
Feature:	Roman flue feature, context 10060
Location:	Longitude 1.8° W, Latitude 51.6° N
Number of specimens (taken/used in mean):	12/-
AF Demagnetisation Applied:	0-100mT (see text and Table 13)
Distortion Correction Applied:	None
Declination (at Meriden):	N/A
Inclination (at Meriden):	N/A
Alpha-95:	N/A
k:	N/A
Date range (95% confidence):	Not datable using archaeomagnetism
Independent date estimate:	Roman
Quality as calibration data:	N/A

TABLES

Table 1: NRM measurements of specimens and measurements after partial AF demagnetisation for feature 1GW. J = magnitude of magnetisation vector; AF = peak alternating field strength of demagnetising field; R = specimen rejected from mean calculation.

Specimen	NRM Measurements				After Partial Demagnetisation				
	Material	Dec°	Inc°	J(mAm^{-1})	AF(mT)	Dec°	Inc°	J(mAm^{-1})	R
1GW01	Stone	-15.6	66.2	13515.4	100.0	-17.2	67.9	1.4	
1GW02	Stone	-11.8	63.5	16237.1	100.0	-15.3	63.7	0.9	
1GW03	Stone	-17.1	59.4	16267.9	100.0	-16.2	60.0	1.3	
1GW04	Stone	-10.9	66.9	18169.9	100.0	-8.1	66.6	1.1	
1GW05	Stone	71.0	9.5	12215.1	100.0	74.8	2.2	1.9	R
1GW06	Stone	62.1	19.3	9042.4	100.0	66.1	10.6	1.8	R
1GW07	Stone	23.9	43.8	8850.1	100.0	11.0	48.0	0.8	
1GW08	Stone	15.8	49.9	14803.4	100.0	14.2	51.3	1.8	
1GW09	Stone	15.5	47.4	13391.0	100.0	9.7	53.2	1.9	
1GW11	Stone	-2.3	53.5	3114.1	100.0	-4.5	55.7	1.5	
1GW12	Stone	-13.6	48.3	17.6	100.0	-13.6	52.6	1.4	
1GW13	Stone	-7.9	62.0	76.3	100.0	-5.7	57.7	1.4	
1GW14	Stone	-10.9	61.9	181.2	100.0	-11.8	60.1	2.0	
1GW15	Stone	-4.2	56.9	95.0	15.0	-5.1	54.6	1.2	
1GW16	Stone	-22.8	-79.8	57.4	100.0	15.3	-78.9	0.8	R
1GW17	Stone	5.1	-82.8	154.5	100.0	1.7	-82.4	1.3	R
1GW18	Stone	-8.8	-83.7	137.0	100.0	-3.6	-81.7	1.4	R
1GW21	Stone	-10.9	25.6	16821.2	100.0	-12.0	16.7	1.0	R
1GW22	Stone	-9.7	26.4	17022.1	100.0	-19.0	3.4	1.6	R

Table 2: Incremental partial demagnetisation measurements for specimens 1GW01, 1GW02 and 1GW03.

AF(mT)	1GW01			1GW02			1GW03		
	Dec°	Inc°	J(mAm^{-1})	Dec°	Inc°	J(mAm^{-1})	Dec°	Inc°	J(mAm^{-1})
0.0	-17.3	68.0	15337.1	-14.1	63.8	17567.8	-16.4	59.6	18674.5
1.0	-17.6	67.6	15181.6	-14.2	63.4	17499.6	-16.3	59.1	18582.6
2.5	-17.8	67.4	14986.7	-14.0	63.3	17343.7	-15.6	59.1	18577.4
5.0	-18.3	67.1	14680.2	-13.1	63.0	16826.5	-16.1	58.7	17978.3
7.5	-19.1	66.9	13976.2	-13.7	62.9	16018.2	-15.3	58.8	17121.9
10.0	-19.1	66.6	13231.3	-13.5	63.0	15159.3	-14.7	58.5	16131.0
15.0	-19.7	66.7	11310.2	-13.0	63.0	12933.7	-14.3	58.2	13487.8
20.0	-20.2	66.4	9555.4	-13.2	63.0	10932.7	-13.9	58.1	11988.5
30.0	-20.5	65.8	7120.1	-12.5	62.5	8114.4	-	-	-
50.0	-20.6	65.1	4571.5	-11.8	62.4	5209.3	-15.5	56.5	6086.7
75.0	-23.0	65.0	2966.8	-10.7	61.4	3500.0	-15.8	54.6	4085.0
100.0	-17.3	67.7	2042.1	-0.9	60.7	2514.8	-13.8	56.4	2808.0

Table 3: Incremental partial demagnetisation measurements for specimens 1GW04, 1GW05 and 1GW06.

AF(mT)	1GW04			1GW05			1GW06		
	Dec°	Inc°	J(mAm^{-1})	Dec°	Inc°	J(mAm^{-1})	Dec°	Inc°	J(mAm^{-1})
0.0	-7.5	66.4	20422.0	71.0	9.0	13923.5	59.8	19.1	9769.2
1.0	-8.1	66.4	20298.0	70.6	8.9	13886.9	60.0	18.7	9862.1
2.5	-8.8	66.3	20102.7	70.4	8.7	13958.4	60.0	18.1	9930.8
5.0	-8.2	66.2	19612.6	70.9	7.8	13800.4	60.1	16.9	9936.1
7.5	-8.5	66.4	18720.4	71.8	6.6	13549.9	61.0	15.6	9867.5
10.0	-9.0	66.5	17693.1	72.3	5.7	13192.4	61.7	14.2	9610.4
15.0	-8.1	67.0	15700.8	72.6	4.7	12123.6	63.4	12.8	8759.3
20.0	-8.2	67.0	13755.3	71.9	4.6	10831.6	63.4	12.3	7817.8
30.0	-8.6	67.4	10719.0	71.0	5.6	8677.5	63.9	12.3	6256.8
50.0	-9.8	65.8	7193.9	68.7	8.3	5686.9	62.4	13.8	4144.1
75.0	-8.3	66.2	4821.7	63.9	13.0	3472.9	57.5	16.9	2675.2
100.0	-7.6	63.1	3487.9	64.7	16.9	2422.5	52.9	19.2	1756.2

Table 4: Incremental partial demagnetisation measurements for specimens 1GW07, 1GW08 and 1GW09.

AF(mT)	1GW07			1GW08			1GW09		
	Dec°	Inc°	J(mAm^{-1})	Dec°	Inc°	J(mAm^{-1})	Dec°	Inc°	J(mAm^{-1})
0.0	23.5	43.7	10148.0	19.4	50.4	16971.2	13.7	47.0	14875.7
1.0	24.0	43.5	10103.6	19.5	50.3	16901.6	14.5	44.4	15350.6
2.5	24.6	43.1	10016.4	18.8	50.1	16778.1	14.0	49.2	15091.5
5.0	25.2	42.3	9763.8	16.3	49.5	16270.5	13.9	48.8	14852.8
7.5	25.8	42.0	9384.8	17.2	49.0	15858.5	13.9	48.5	14364.6
10.0	26.5	41.5	8900.8	17.9	48.6	15099.0	14.3	48.1	13792.3
15.0	28.4	40.6	7817.8	19.4	48.1	13324.4	15.1	47.4	12249.8
20.0	28.3	40.3	6875.7	19.8	47.5	11588.6	15.7	46.7	10765.6
30.0	30.0	38.5	5407.1	19.8	46.3	9123.5	16.3	45.9	8601.0
50.0	29.2	38.4	3554.9	22.5	45.2	6079.6	17.4	45.2	5692.0
75.0	24.7	40.0	2225.2	16.2	46.3	3726.9	18.4	45.5	3484.2
100.0	21.3	40.2	1507.9	15.0	44.1	2507.0	14.3	47.9	2182.8

Table 5: Incremental partial demagnetisation measurements for specimens 1GW11, 1GW12 and 1GW13.

AF(mT)	1GW11			1GW12			1GW13		
	Dec°	Inc°	J(mAm^{-1})	Dec°	Inc°	J(mAm^{-1})	Dec°	Inc°	J(mAm^{-1})
0.0	-6.0	56.3	3428.1	-21.4	56.2	28.0	-7.0	59.6	109.6
1.0	-5.0	55.6	3418.4	-20.4	55.6	27.4	-6.0	58.2	109.5
2.5	-4.6	55.1	3397.1	-21.0	53.7	26.0	-6.7	57.7	108.0
5.0	-4.4	54.7	3289.7	-19.3	53.9	25.2	-6.9	57.4	104.5
7.5	-4.4	54.1	3138.1	-18.0	52.5	23.5	-7.2	57.0	100.8
10.0	-4.2	53.8	2931.3	-18.4	53.1	22.7	-6.7	56.7	95.3
15.0	-3.9	53.4	2452.3	-18.7	50.5	19.5	-7.2	56.4	84.1
20.0	-4.6	53.2	2035.8	-21.7	52.9	17.5	-6.9	56.6	72.0
30.0	-4.5	52.7	1460.9	-21.3	52.4	14.3	-7.4	56.5	54.2
50.0	-4.9	52.1	868.1	-30.4	52.5	7.3	-9.4	55.7	33.8
75.0	-5.0	50.2	593.2	-60.6	50.1	2.6	-9.7	55.8	17.8
100.0	-4.4	50.3	467.2	-118.3	-19.4	1.6	-19.2	58.8	8.8

Table 6: Incremental partial demagnetisation measurements for specimens 1GW14, 1GW15 and 1GW16.

AF(mT)	1GW14			1GW15			1GW16		
	Dec°	Inc°	J(mAm⁻¹)	Dec°	Inc°	J(mAm⁻¹)	Dec°	Inc°	J(mAm⁻¹)
0.0	-14.4	60.3	183.8	-1.7	59.6	99.2	-9.7	-83.9	47.5
1.0	-13.9	60.1	180.8	-1.6	59.2	99.3	-12.0	-84.0	48.6
2.5	-12.7	59.9	178.3	-2.5	58.5	97.8	-11.8	-84.1	48.4
5.0	-12.1	59.5	169.6	-2.7	58.2	94.9	-3.3	-83.7	48.3
7.5	-11.1	58.9	160.1	-2.8	58.0	91.5	-8.1	-84.9	46.8
10.0	-10.9	58.6	147.1	-2.6	58.0	86.6	-7.6	-84.1	44.1
15.0	-11.0	58.4	125.5	-2.3	58.6	77.0	-12.4	-85.4	38.4
20.0	-10.4	57.7	106.5	-	-	-	-17.3	-86.5	33.4
30.0	-10.4	57.7	79.3	-	-	-	-19.3	-86.2	25.1
50.0	-13.0	57.4	50.3	-	-	-	-94.8	-86.2	15.4
75.0	-16.9	56.2	28.0	-	-	-	-136.4	-77.9	9.5
100.0	-21.3	57.4	14.9	-	-	-	-132.5	-77.1	7.0

Table 7: Incremental partial demagnetisation measurements for specimens 1GW17 and 1GW18.

AF(mT)	1GW17			1GW18		
	Dec°	Inc°	J(mAm⁻¹)	Dec°	Inc°	J(mAm⁻¹)
0.0	-0.5	-82.7	124.0	-8.2	-82.4	92.9
1.0	-6.7	-83.3	124.3	-7.4	-82.6	93.2
2.5	-7.2	-83.9	123.8	-8.5	-82.9	92.5
5.0	-6.3	-83.5	121.8	-5.5	-83.0	91.2
7.5	-3.8	-83.4	118.8	-1.1	-82.7	88.9
10.0	-6.5	-83.8	113.9	-5.4	-82.5	84.7
15.0	-3.1	-83.6	104.1	-7.3	-83.8	77.7
20.0	-3.9	-84.6	93.6	0.5	-82.7	69.4
30.0	-10.2	-84.7	74.7	-6.8	-83.2	54.6
50.0	-25.4	-85.4	45.1	-13.8	-85.6	33.2
75.0	-52.2	-85.7	25.7	-29.0	-85.4	18.9
100.0	-90.3	-83.8	14.6	-80.7	-87.4	11.0

Table 8: Incremental partial demagnetisation measurements for specimens 1GW21 and 1GW22.

AF(mT)	1GW21			1GW22		
	Dec°	Inc°	J(mAm⁻¹)	Dec°	Inc°	J(mAm⁻¹)
0.0	-9.4	26.2	19103.2	-8.2	25.3	18892.7
1.0	-9.3	26.4	19080.2	-9.7	25.2	18844.4
2.5	-9.4	26.1	18883.0	-9.5	24.7	18616.8
5.0	-9.5	25.3	18306.1	-10.9	22.9	17476.9
7.5	-9.7	23.6	17031.3	-12.1	20.0	15333.6
10.0	-10.8	21.4	15389.6	-13.5	15.2	12337.2
15.0	-11.8	16.9	11400.1	-15.4	9.2	8391.0
20.0	-11.6	15.5	8403.6	-16.7	8.7	6102.8
30.0	-10.9	16.4	5198.4	-14.6	12.7	4102.1
50.0	-11.7	15.5	2869.1	-13.2	16.5	2775.7
75.0	-10.8	14.9	1492.9	-11.9	19.2	2146.9
100.0	-8.1	14.9	887.0	-10.5	21.6	1808.6

Table 9: Assessment of the range of demagnetisation values over which each specimen attained its maximum directional consistency and linearity for feature 1GW. Consistency is calculated using the method of Tarling and Symons (1967) and linearity using the method of Kirshvink (1980). Min and Max indicate the range of demagnetisation values in mT over which each statistic was calculated and N is the number of consecutive measurements this represents. MCI is the maximum value of Tarling and Symons' consistency index found for the specimen (over 2 for a stable magnetisation). MAD is Kirshvink's maximum angular deviation (less than 2° indicates linearity). In each case, declination and inclination values are for the mean direction calculated from all demagnetisation measurements in the range indicated.

Specimen	Consistency						Linearity					
	Min	Max	N	MCI	Dec°	Inc°	Min	Max	N	MAD°	Dec°	Inc°
1GW01	7.5	15.0	3	42.2	-19.3	66.7	0.0	100.0	12	1.4	-17.2	67.9
1GW02	5.0	20.0	5	87.6	-13.3	63.0	0.0	100.0	12	0.9	-15.3	63.7
1GW03	10.0	20.0	3	33.8	-14.3	58.3	0.0	100.0	11	1.3	-16.2	60.0
1GW04	0.0	75.0	11	53.5	-8.5	66.5	0.0	100.0	12	1.1	-8.1	66.6
1GW05	10.0	30.0	4	15.7	72.0	5.2	10.0	100.0	7	1.9	74.8	2.2
1GW06	15.0	30.0	3	30.4	63.6	12.5	15.0	100.0	6	1.8	66.1	10.6
1GW07	15.0	50.0	4	14.2	29.0	39.5	5.0	15.0	4	0.8	11.0	48.0
1GW08	0.0	2.5	3	17.5	19.2	50.3	7.5	50.0	6	1.8	14.2	51.3
1GW09	30.0	75.0	3	26.1	17.4	45.5	2.5	30.0	7	1.9	9.7	53.2
1GW11	20.0	50.0	3	30.7	-4.7	52.7	1.0	100.0	11	1.5	-4.5	55.7
1GW12	2.5	30.0	7	11.4	-19.8	52.7	20.0	100.0	5	1.4	-13.6	52.6
1GW13	15.0	30.0	3	71.6	-7.2	56.5	1.0	100.0	11	1.4	-5.7	57.7
1GW14	7.5	15.0	3	33.7	-11.0	58.6	1.0	100.0	11	2.0	-11.8	60.1
1GW15	5.0	10.0	3	55.7	-2.7	58.1	7.5	15.0	3	1.2	-5.1	54.6
1GW16	0.0	2.5	3	29.9	-11.2	-84.0	30.0	75.0	3	0.8	15.3	-78.9
1GW17	1.0	15.0	6	39.5	-5.6	-83.6	0.0	100.0	12	1.3	1.7	-82.4
1GW18	0.0	30.0	9	29.6	-5.5	-82.9	0.0	100.0	12	1.4	-3.6	-81.7
1GW21	0.0	2.5	3	31.0	-9.4	26.2	15.0	100.0	6	1.0	-12.0	16.7
1GW22	50.0	100.0	3	7.8	-11.9	19.1	20.0	100.0	5	1.6	-19.0	3.4

Table 10: NRM measurements of specimens for feature 2GW. J = magnitude of magnetisation vector.

Specimen	NRM Measurements			
	Material	Dec°	Inc°	J(mAm^{-1})
2GW01	Stone	-150.3	-32.2	2.0
2GW03	Stone	-66.2	-30.6	1.1
2GW04	Stone	-121.7	-8.8	0.7
2GW05	Stone	-99.9	-20.8	1.1
2GW06	Stone	9.3	-19.5	3.8
2GW07	Clay	-117.2	61.9	1.9
2GW08	Clay	-23.4	76.6	64.7
2GW09	Clay	-24.8	3.8	22.4
2GW10	Clay	-29.3	70.7	6.8
2GW11	Clay	-33.5	-2.5	141.7
2GW12	Clay	-137.6	-19.6	136.8

Table 11: Incremental partial demagnetisation measurements for specimens 2GW08 and 2GW09.

AF(mT)	2GW08			2GW09		
	Dec°	Inc°	J(mAm^{-1})	Dec°	Inc°	J(mAm^{-1})
0.0	-48.7	80.1	62.0	-25.6	-0.6	21.8
1.0	-43.2	78.5	60.6	-26.7	-0.5	21.7
2.5	-38.6	77.1	59.2	-26.0	0.9	21.1
5.0	-31.5	74.6	50.7	-28.6	-1.3	21.1
7.5	-33.6	73.1	45.0	-27.4	0.4	20.4
10.0	-37.3	72.1	33.6	-28.5	-1.4	19.9
15.0	-48.9	72.7	20.9	-27.4	-2.3	19.4
20.0	-54.2	72.7	13.5	-29.0	-4.2	18.9
30.0	-89.7	67.2	7.0	-27.1	-5.6	17.7
50.0	-121.0	46.9	3.7	-30.3	-10.2	12.4
75.0	-	-	-	-34.7	-5.1	7.8
100.0	-	-	-	-53.8	-26.0	4.1

Table 12: Incremental partial demagnetisation measurements for specimens 2GW11 and 2GW12.

AF(mT)	2GW11			2GW12		
	Dec°	Inc°	J(mAm^{-1})	Dec°	Inc°	J(mAm^{-1})
0.0	-38.2	-3.2	127.7	-157.0	-37.5	116.9
1.0	-39.2	-4.5	132.5	-156.5	-37.5	120.0
2.5	-39.2	-5.8	136.0	-153.8	-37.5	122.4
5.0	-39.4	-8.3	138.1	-151.5	-40.2	124.4
7.5	-40.8	-10.2	140.2	-149.6	-41.3	127.8
10.0	-41.9	-11.5	140.0	-147.2	-41.3	130.0
15.0	-43.1	-13.6	137.4	-145.2	-41.7	134.1
20.0	-43.9	-14.7	133.8	-142.7	-41.6	135.7
30.0	-44.6	-15.3	124.3	-139.9	-41.2	130.0
50.0	-45.9	-17.4	100.3	-140.7	-41.6	99.6
75.0	-44.7	-17.6	67.9	-143.0	-40.6	60.9
100.0	-47.8	-16.9	36.7	-144.2	-38.1	24.8

Table 13: Assessment of the range of demagnetisation values over which each specimen attained its maximum directional consistency and linearity for feature 2GW. Consistency is calculated using the method of Tarling and Symons (1967) and linearity using the method of Kirshvink (1980). Min and Max indicate the range of demagnetisation values in mT over which each statistic was calculated and N is the number of consecutive measurements this represents. MCI is the maximum value of Tarling and Symons' consistency index found for the specimen (over 2 for a stable magnetisation). MAD is Kirshvink's maximum angular deviation (less than 2^{o} indicates linearity). In each case, declination and inclination values are for the mean direction calculated from all demagnetisation measurements in the range indicated.

Specimen	Consistency						Linearity					
	Min	Max	N	MCI	Dec°	Inc°	Min	Max	N	MAD°	Dec°	Inc°
2GW08	5.0	10.0	3	4.7	-34.3	73.3	7.5	50.0	6	1.2	-23.2	71.7
2GW09	0.0	15.0	7	7.7	-27.2	-0.7	-	-	-	-	-	-
2GW11	30.0	100.0	4	15.0	-45.7	-16.8	20.0	50.0	3	0.9	-38.5	-6.6
2GW12	20.0	75.0	4	19.0	-141.6	-41.3	30.0	100.0	4	1.1	-138.6	-42.1

APPENDIX: STANDARD PROCEDURES FOR SAMPLING AND MEASUREMENT

The principles underlying the archaeomagnetic dating method have been described by Linford (2004) and the procedures employed are described in English Heritage (2006). These notes summarise the most important points.

1) Sampling

One of three sampling techniques is employed depending on the consistency of the material (Clark *et al.* 1988 ; English Heritage 2006):

a) Consolidated materials: Rock and fired clay specimens are collected by the disc method. Several small levelled plastic discs are glued to the feature, marked with an orientation line related to True North, then removed with a small piece of the material attached.
b) Unconsolidated materials: Sediments are collected by the tube method. Small pillars of the material are carved out from a prepared platform, then encapsulated in levelled plastic tubes using plaster of Paris. The orientation line is then marked on top of the plaster.
c) Plastic materials: Waterlogged clays and muds are sampled in a similar manner to method 1b) above; however, the levelled plastic tubes are pressed directly into the material to be sampled.

2) Physical Analysis

a) Magnetic remanences are measured using a slow speed spinner fluxgate magnetometer (Molyneux 1971 ; see also Tarling 1983, p84; Thompson and Oldfield 1986).
b) Partial demagnetisation is achieved using the alternating magnetic field method (Tarling 1983, p91; Thompson and Oldfield 1986, p59), to remove viscous magnetic components if necessary. Demagnetising fields are measured in millitesla (mT), figures quoted being for the peak value of the field.

3) Remanent Field Direction

a) The remanent field direction of a specimen is expressed as two angles, declination (Dec) and inclination (Inc), both quoted in degrees. Declination represents the bearing of the field relative to true north, angles to the east being positive; inclination represents the angle of dip of this field.
b) Aitken and Hawley (1971) have shown that the angle of inclination in measured specimens is likely to be distorted owing to magnetic refraction. The phenomenon is

not well understood but is known to depend on the position the specimens occupied within the structure. The corrections recommended by Aitken and Hawley are applied, where appropriate, to measured inclinations, in keeping with the practice of Clark, Tarling and Noel (1988).

c) Individual remanent field directions are combined to produce the mean remanent field direction using the statistical method developed by R. A. Fisher (1953). The quantity α_{95}, "alpha-95", is quoted with mean field directions and is a measure of the precision of the determination (see Aitken 1990, p247). It is analogous to the standard error statistic for scalar quantities; hence the smaller its value, the better the precision of the date.
d) For the purposes of comparison with standardised UK calibration data, remanent field directions are adjusted to the values they would have had if the feature had been located at Meriden, a standard reference point. The adjustment is done using the method suggested by Noel (Tarling 1983, p116).

4) Calibration

a) Material less than 3000 years old is dated using the archaeomagnetic calibration curve compiled by Clark, Tarling and Noel (1988).
b) Older material is dated using the lake sediment data compiled by Thompson and Turner (Thompson and Turner 1979 ; Turner and Thompson 1981).
c) Dates are normally given at the 95% confidence level. However, the quality of the measurement and the estimated reliability of the calibration curve for the period in question are not taken into account, so this figure is only approximate. Owing to crossovers and contiguities in the curve, alternative dates are sometimes given. It may be possible to select the correct alternative using independent dating evidence.
d) As the thermoremanent effect is reset at each heating, all dates for fired material refer to the final heating.

REFERENCES

Aitken, M J 1990 *Science-based dating in archaeology*, London, Longman.

Aitken, M J and Hawley, H N 1971 'Archaeomagnetism: evidence for refraction in kiln structures'. *Archaeometry*, 13, 83-5.

Beck, M E, Jr. 1983 'Comment on `Determination of the angle of a Fisher distribution which will be exceeded with a given probability' by P. L. McFadden'. *Geophysical Journal of the Royal Astronomical Society*, 75, 847-849.

Clark, A J, Tarling, D H and Noël, M 1988 'Developments in Archaeomagnetic Dating in Britain'. *Journal of Archaeological Science*, 15, 645-667.

Corney, M 1997 *Abbey Mead, Groundwell Ridge, Blunsdon St. Andrew, Wiltshire. An Analytical Archaeological Earthwork Survey*, Unpublished report for Swindon Borough Council.

English Heritage 2006 Archaeomagnetic Dating: Guidelines on producing and interpreting archaeomagnetic dates. Swindon, English Heritage.

Fisher, R A 1953 'Dispersion on a sphere'. *Proceedings of the Royal Society of London A*, 217, 295-305.

Kirshvinck, J L 1980 'The least-squares line and plane and the analysis of paleomagentic data'. *Geophysical Journal of the Royal Astronomical Society*, 62, 699-718.

Linford, N 2002 *'Groundwell Ridge, Blunsdon St. Andrew, Swindon: Report on Ground Penetrating Radar Survey, July 2002'.* English Heritage Centre for Archaeology Report Series 83/2002.

Linford, N and Linford, P 2004 'Ground Penetrating Radar Survey over a Roman, Building at Groundwell Ridge, Blunsdon St Andrew, Swindon, UK'. *Archaeological Prospection* (11), 49-55.

Linford, P 1999 *'Abbey Mead, Groundwell Ridge, Blunsdon St. Andrew: Report on Geophysical Survey, 1997'.* English Heritage Ancient Monuments Laboratory report series 15/1999.

Linford, P 2004 'Archaeomagnetic Dating'. *Physics Education*, 39 (2), 145-154.

Linford, P and Martin, L 2002 *'Groundwell Ridge, Blunsdon St. Andrew: Report on Geophysical Surveys, March - April 2002'.* English Heritage Centre for Archaeology report series 44/2002.

Molyneux, L 1971 'A complete result magnetometer for measuring the remanent magnetization of rocks'. *Geophysical Journal of the Royal Astronomical Society*, 24, 429-433.

Phillips, B and Walters, B 1997 *'Blunsdon Ridge, 1997 (BR97) An Archaeological Evaluation, amended edition'.*

Tarling, D H 1983 *Palaeomagnetism: Principles and applications on geology, geophysics and archaeology*, London, Chapman and Hall.

Thompson, R and Oldfield, F 1986 *Environmental Magnetism*, London, Allen and Unwin.

Thompson, R and Turner, G M 1979 'British geomagnetic master curve 10,000-0 yr BP for dating European sediments'. *Geophys. Res. Letters*, 6, 249-252.

Turner, G M and Thompson, R 1981 'Lake sediment record of the geomagnetic secular variation in Britain during Holocene times'. *Geophysical Journal of the Royal Astronomical Society*, 65, 703-725.

Zananiri, I, Batt, C M, Lanos, P, Tarling, D H and Linford, P 2007 'Archaeomagnetic secular variation in the UK during the past 4000 years and its application to archaeomagnetic dating'. *Physics of The Earth and Planetary Interiors*, 160 (2), 97-107.

a)

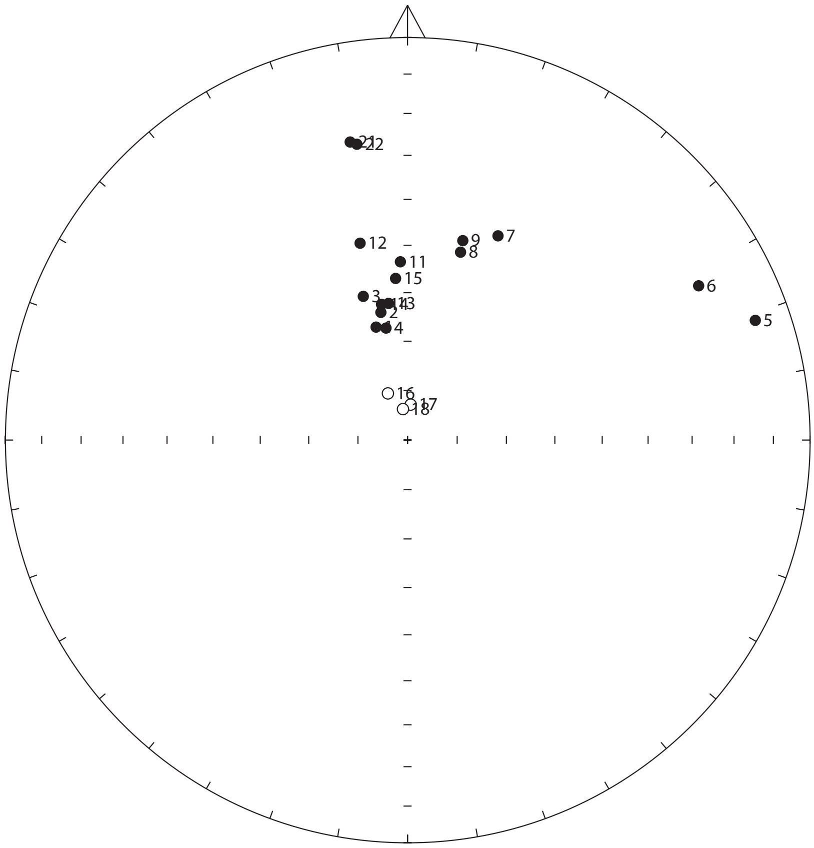

b)

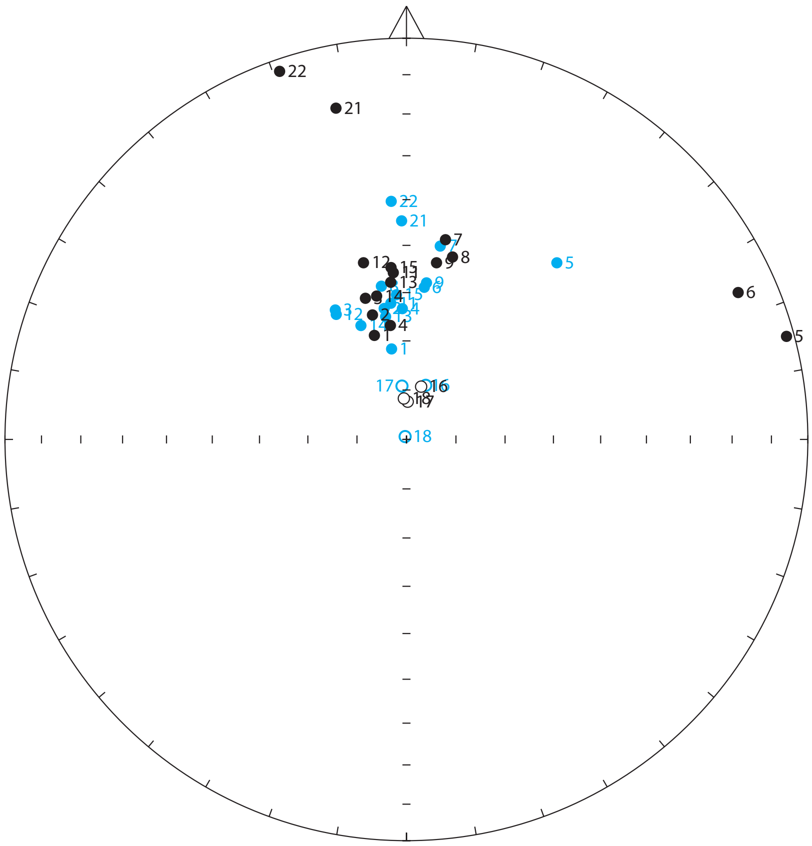

Figure 3: a) Distribution of NRM directions of specimens from feature 1GW represented as an equal area stereogram. In this projection declination increases clockwise with zero being at 12 o'clock while inclination increases from zero at the equator to 90 degrees in the centre of the projection. Open circles represent negative inclinations. b) The directions shown in black represent the distribution of ChRM directions of the same specimens determined after partial demagnetisation to 100 mT while the directions shown in cyan represent the directions of the VRM component at coercivities between 5 and 10 mT.

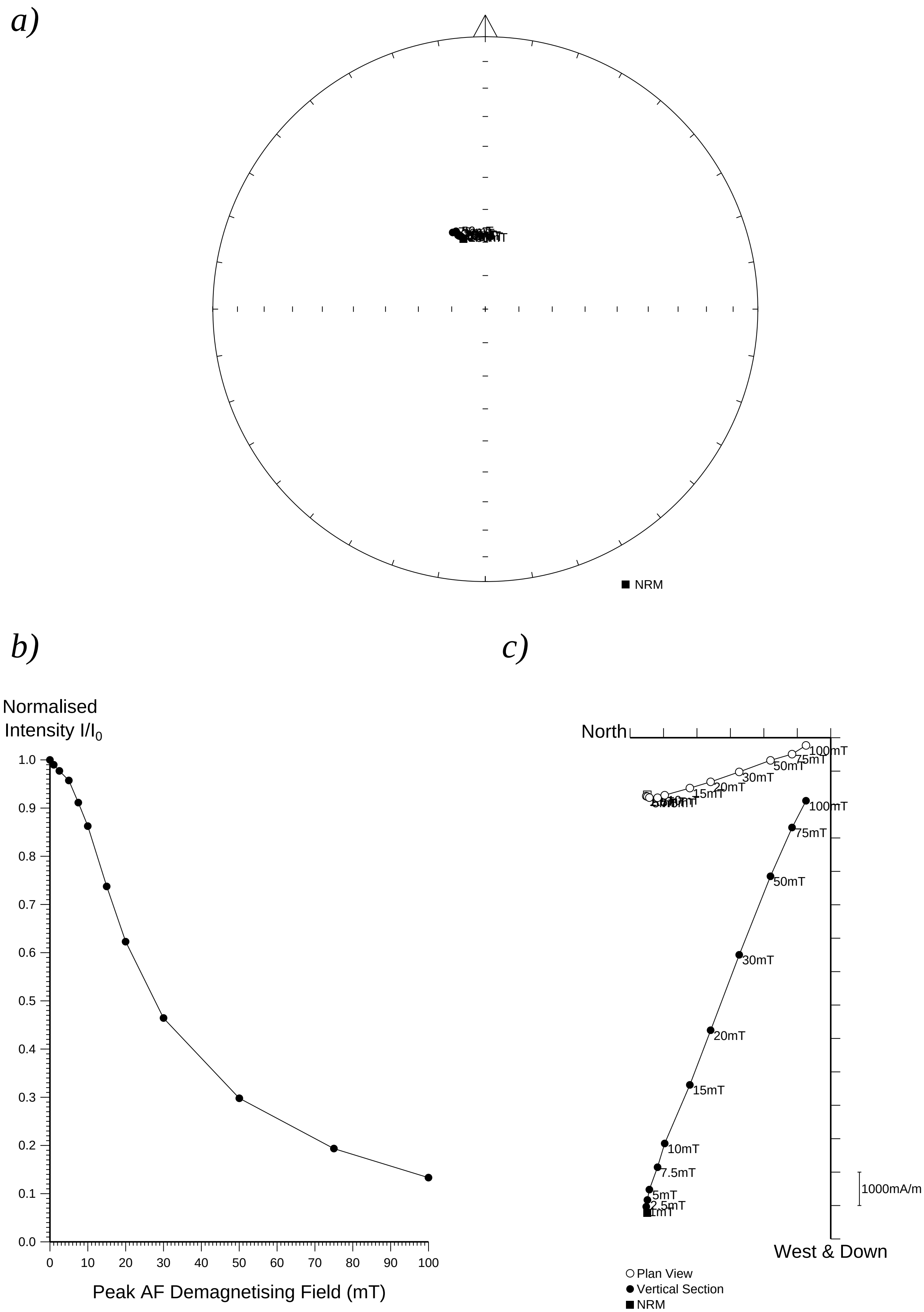

Figure 4: Stepwise AF demagnetisation of sample 1GW01. Diagram a) depicts the variation of the remanent direction as an equal area stereogram (declination increases clockwise, while inclination increases from zero at the equator to 90 degrees at the centre of the projection); b) shows the normalised change in remanence intensity as a function of the demagnetising field; c) shows the changes in both direction and intensity as a vector endpoint projection.

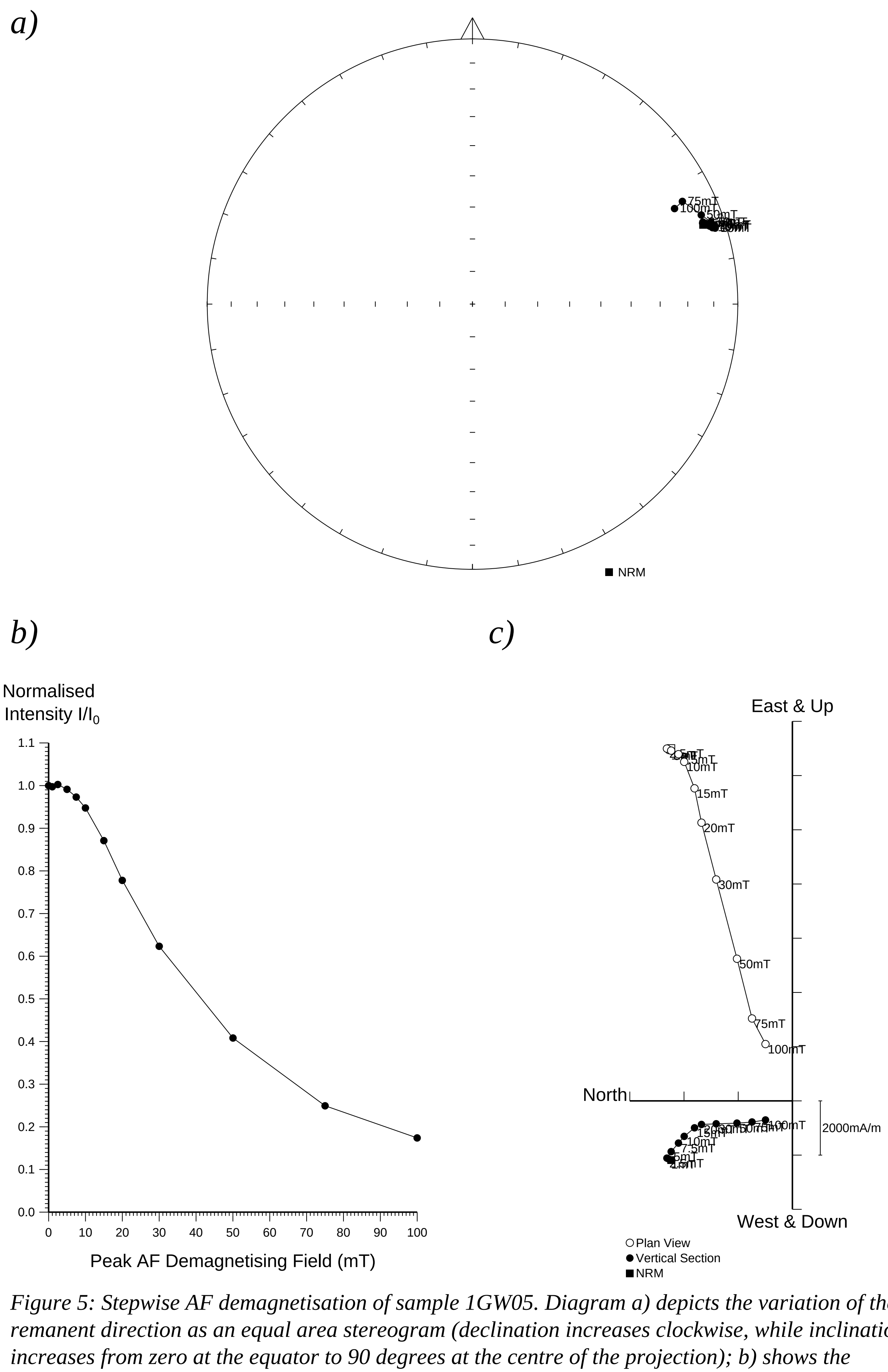

Figure 5: Stepwise AF demagnetisation of sample 1GW05. Diagram a) depicts the variation of the remanent direction as an equal area stereogram (declination increases clockwise, while inclination increases from zero at the equator to 90 degrees at the centre of the projection); b) shows the normalised change in remanence intensity as a function of the demagnetising field; c) shows the changes in both direction and intensity as a vector endpoint projection.

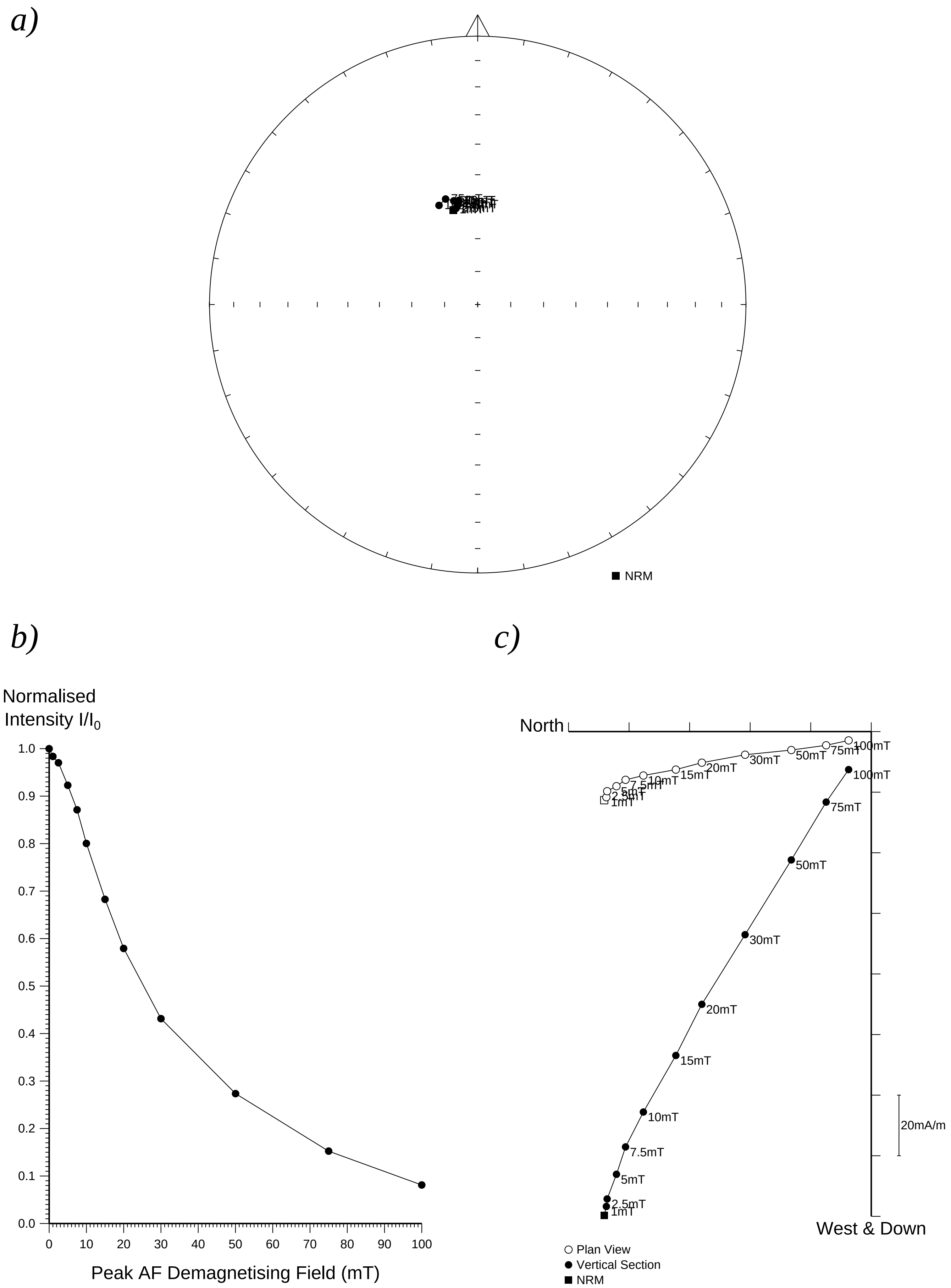

Figure 6: Stepwise AF demagnetisation of sample 1GW14. Diagram a) depicts the variation of the remanent direction as an equal area stereogram (declination increases clockwise, while inclination increases from zero at the equator to 90 degrees at the centre of the projection); b) shows the normalised change in remanence intensity as a function of the demagnetising field; c) shows the changes in both direction and intensity as a vector endpoint projection.

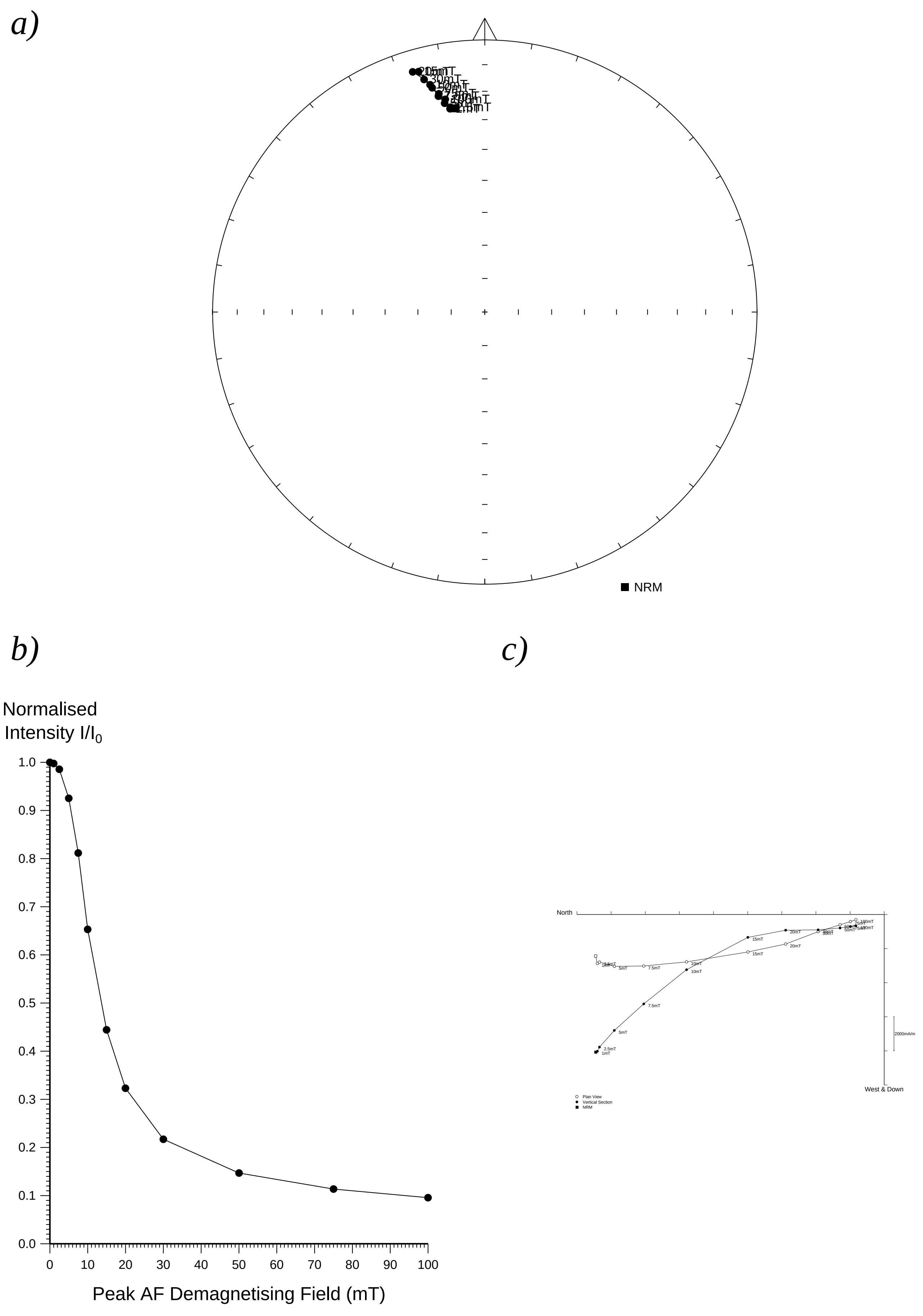

Figure 7: Stepwise AF demagnetisation of sample 1GW22. Diagram a) depicts the variation of the remanent direction as an equal area stereogram (declination increases clockwise, while inclination increases from zero at the equator to 90 degrees at the centre of the projection); b) shows the normalised change in remanence intensity as a function of the demagnetising field; c) shows the changes in both direction and intensity as a vector endpoint projection.

a)

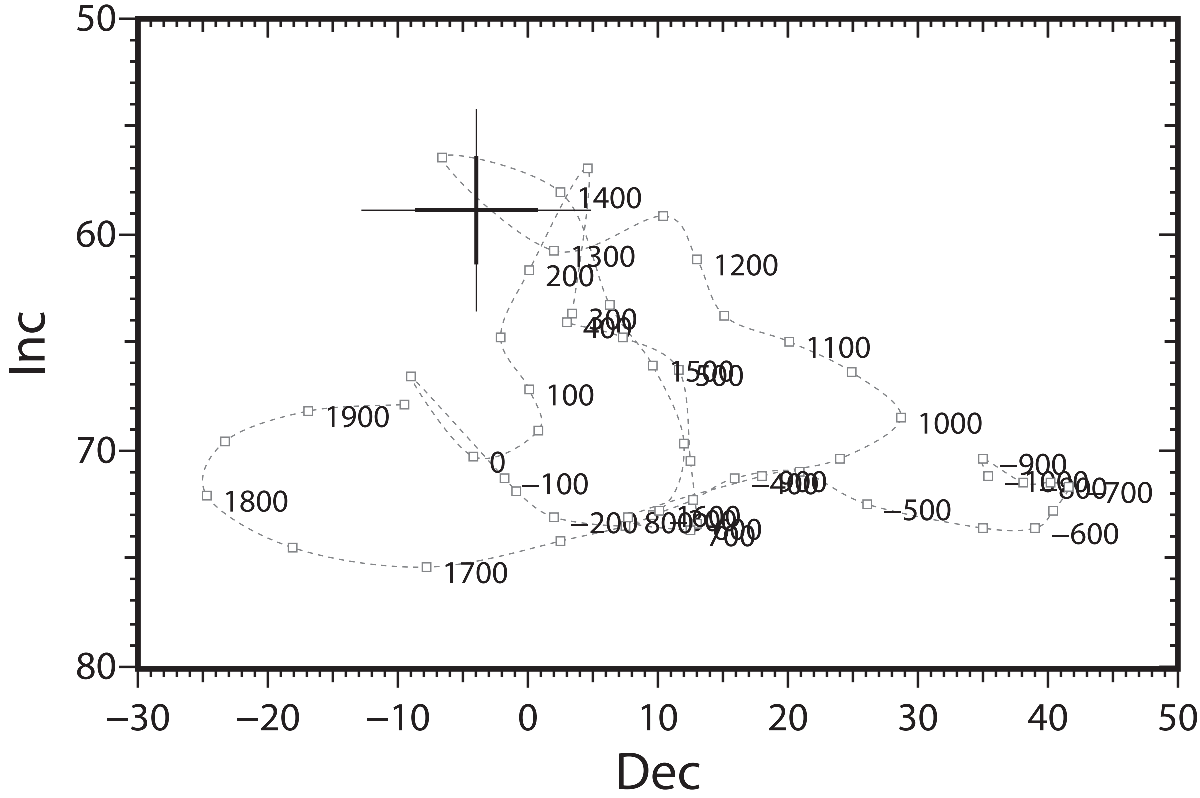

b)

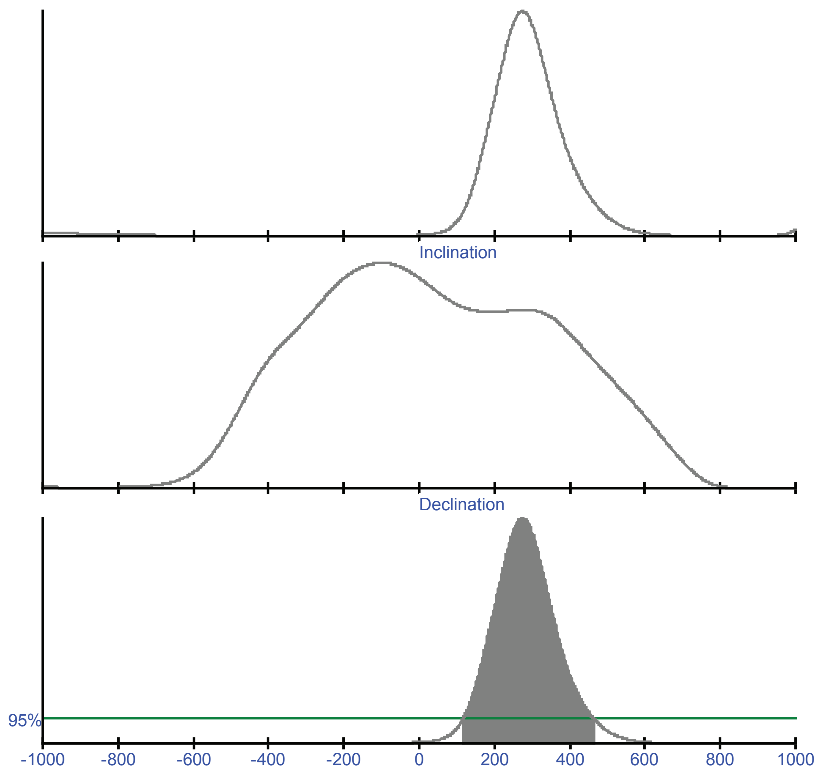

Figure 8: a) Comparison of the mean thermoremanent vector calculated from specimens 01-04, 07-09 and 11-15 from feature 1GW after 100 mT partial demagnetisation with the UK calibration curve of Clark, Tarling and Noel (1988). Thick error bar lines represent 63% confidence limits and narrow lines 95% confidence limits. b) Probability density distributions for the same mean vector when compared to the UK calibration curve of Zananiri et al (2007).

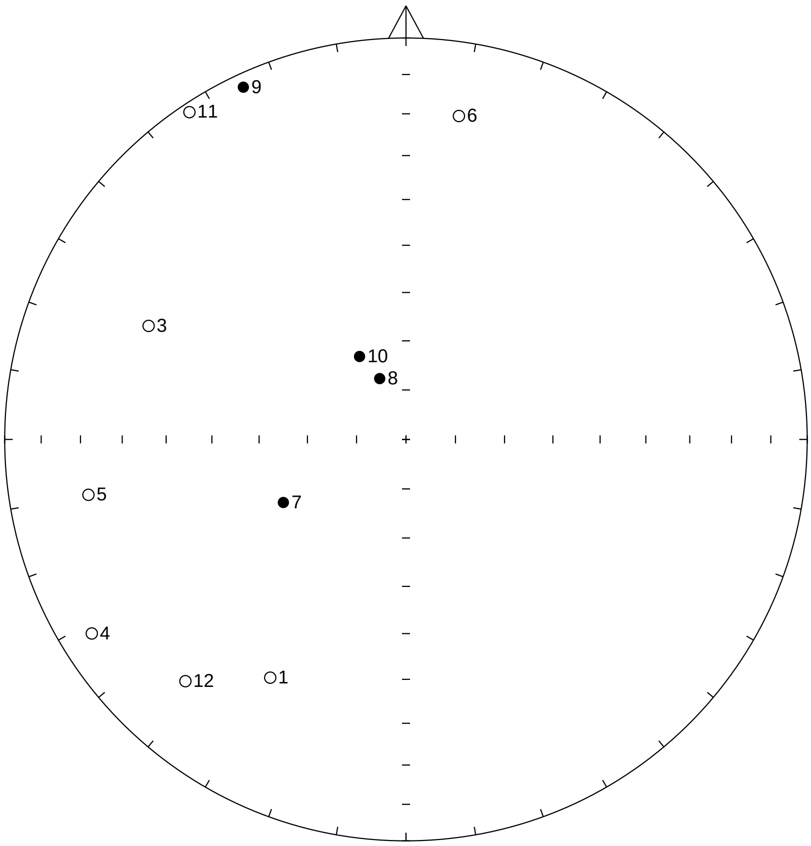

Figure 9: Distribution of NRM directions of samples from feature 2GW represented as an equal area stereogram. In this projection declination increases clockwise with zero being at 12 o'clock while inclination increases from zero at the equator to 90 degrees in the centre of the projection. Open circles represent negative inclinations.

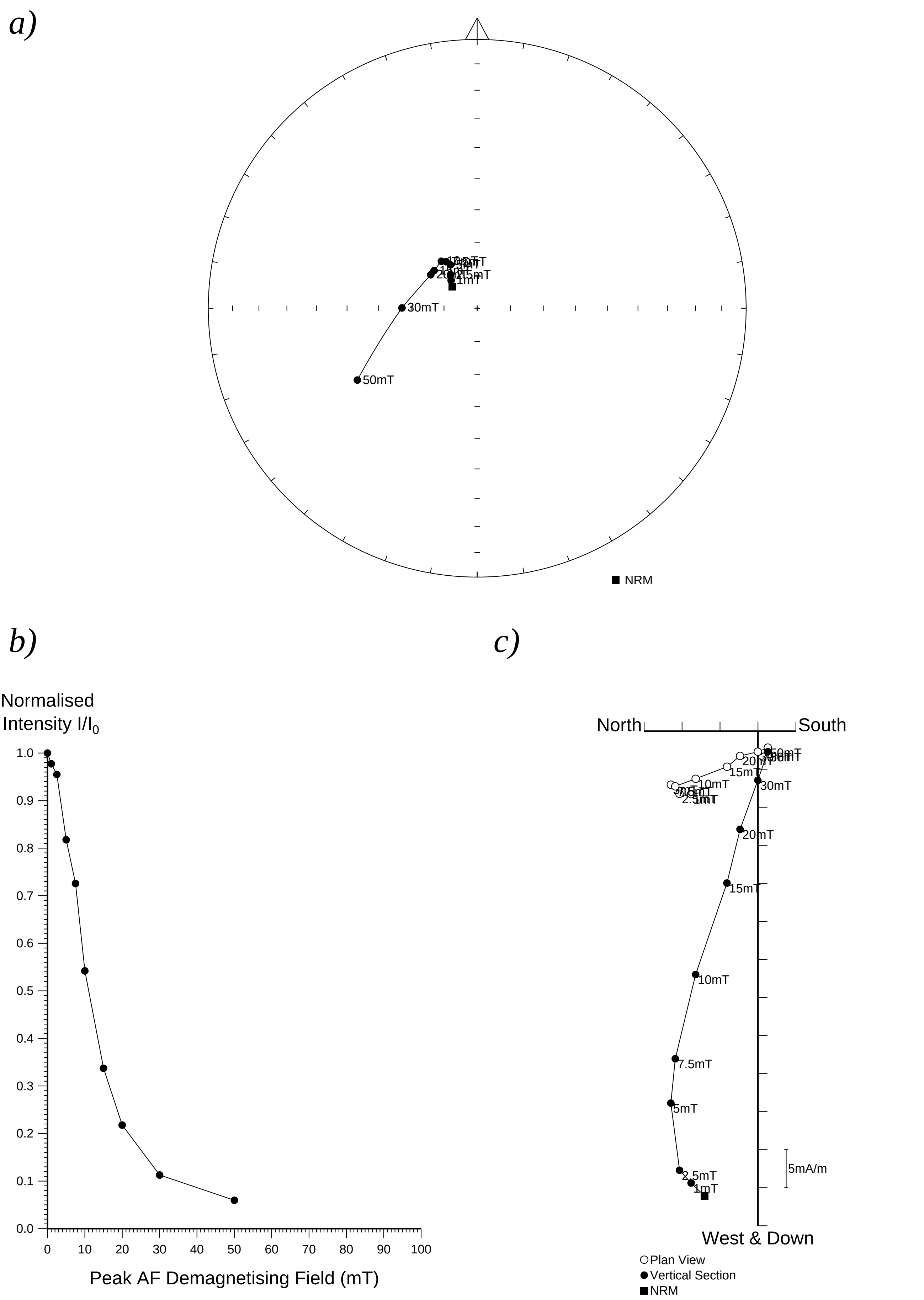

Figure 10: Stepwise AF demagnetisation of sample 2GW08. Diagram a) depicts the variation of the remanent direction as an equal area stereogram (declination increases clockwise, while inclination increases from zero at the equator to 90 degrees at the centre of the projection); b) shows the normalised change in remanence intensity as a function of the demagnetising field; c) shows the changes in both direction and intensity as a vector endpoint projection.

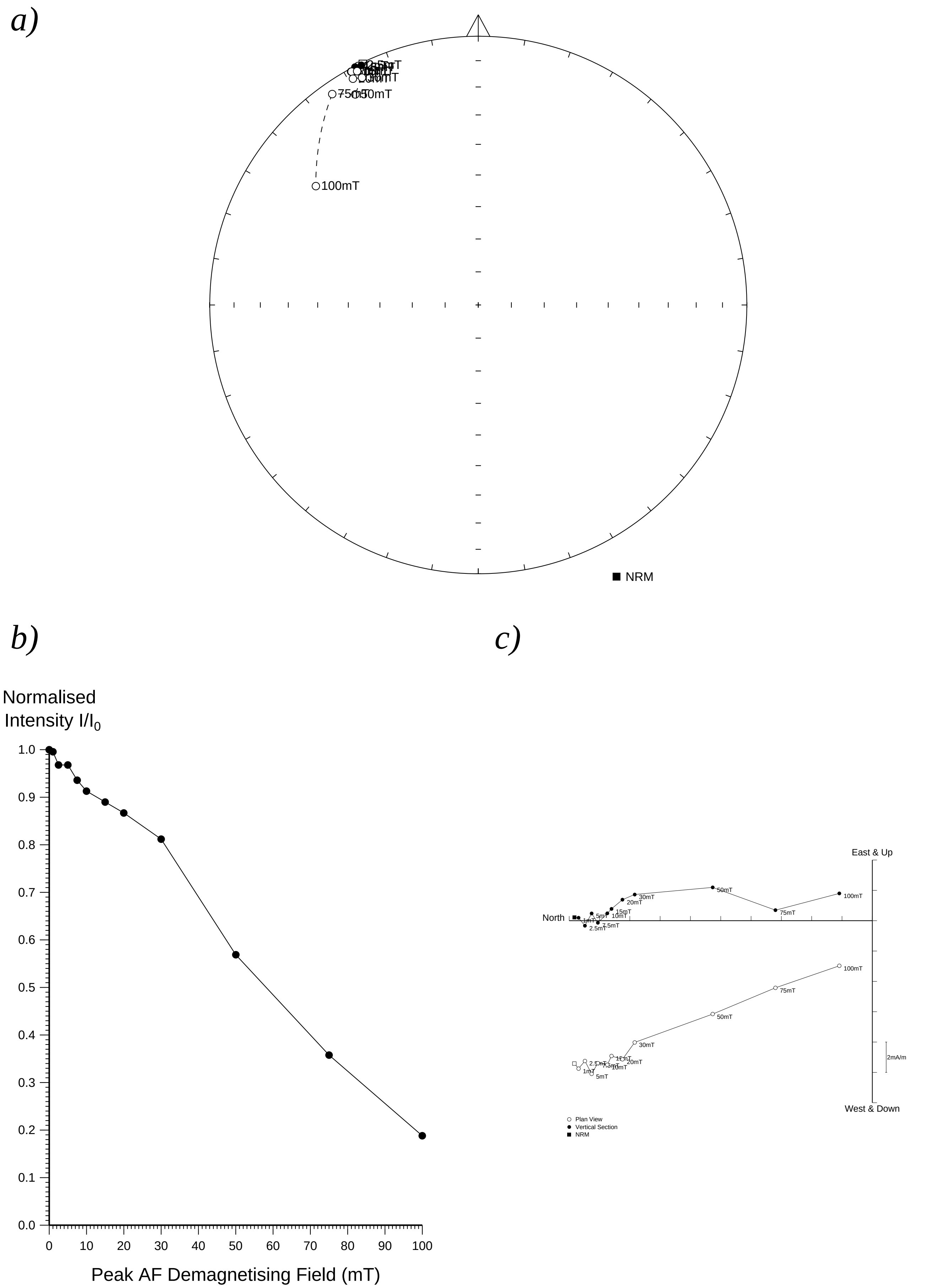

Figure 11: Stepwise AF demagnetisation of sample 2GW09. Diagram a) depicts the variation of the remanent direction as an equal area stereogram (declination increases clockwise, while inclination increases from zero at the equator to 90 degrees at the centre of the projection); b) shows the normalised change in remanence intensity as a function of the demagnetising field; c) shows the changes in both direction and intensity as a vector endpoint projection.

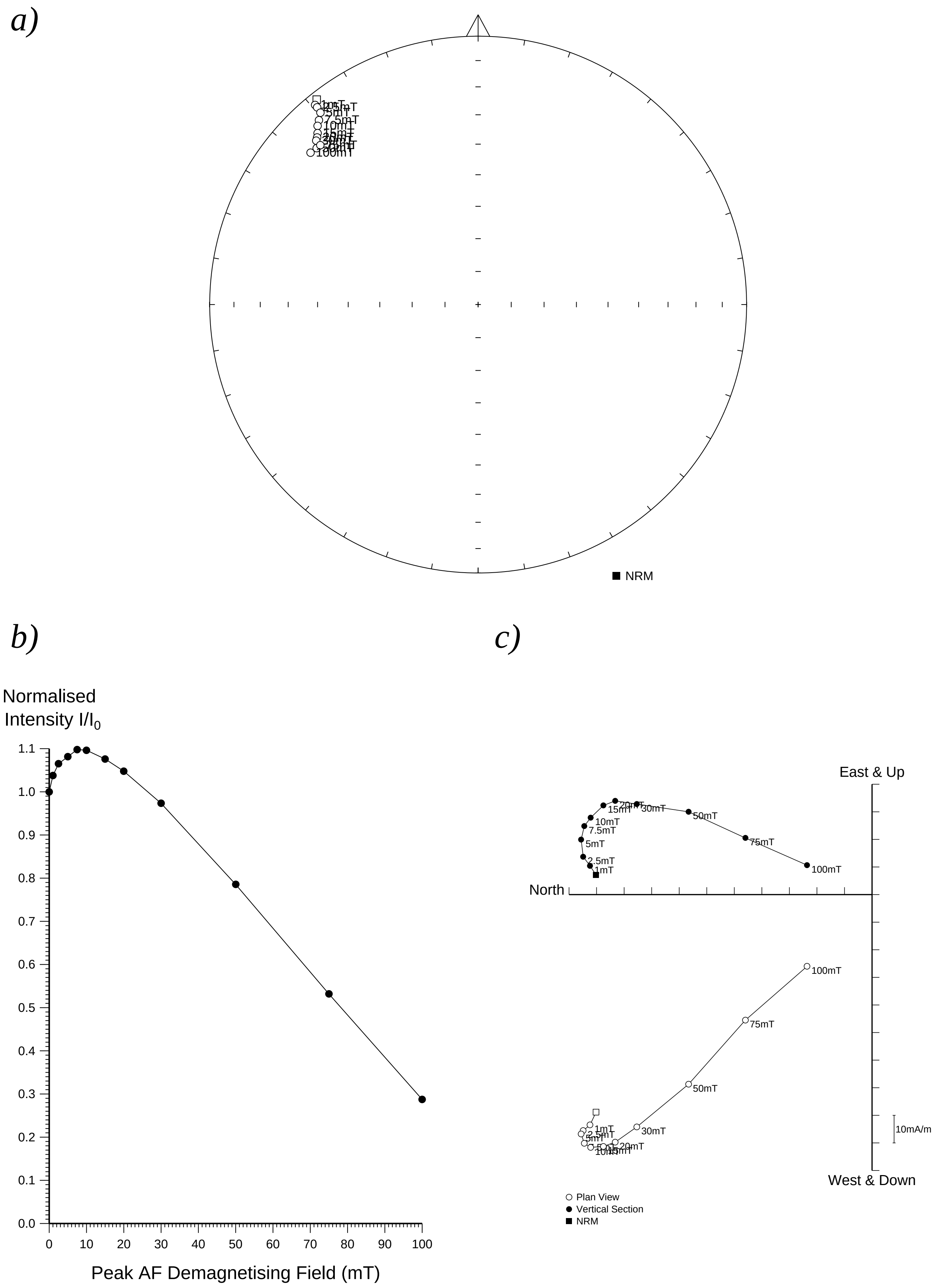

Figure 12: Stepwise AF demagnetisation of sample 2GW11. Diagram a) depicts the variation of the remanent direction as an equal area stereogram (declination increases clockwise, while inclination increases from zero at the equator to 90 degrees at the centre of the projection); b) shows the normalised change in remanence intensity as a function of the demagnetising field; c) shows the changes in both direction and intensity as a vector endpoint projection.

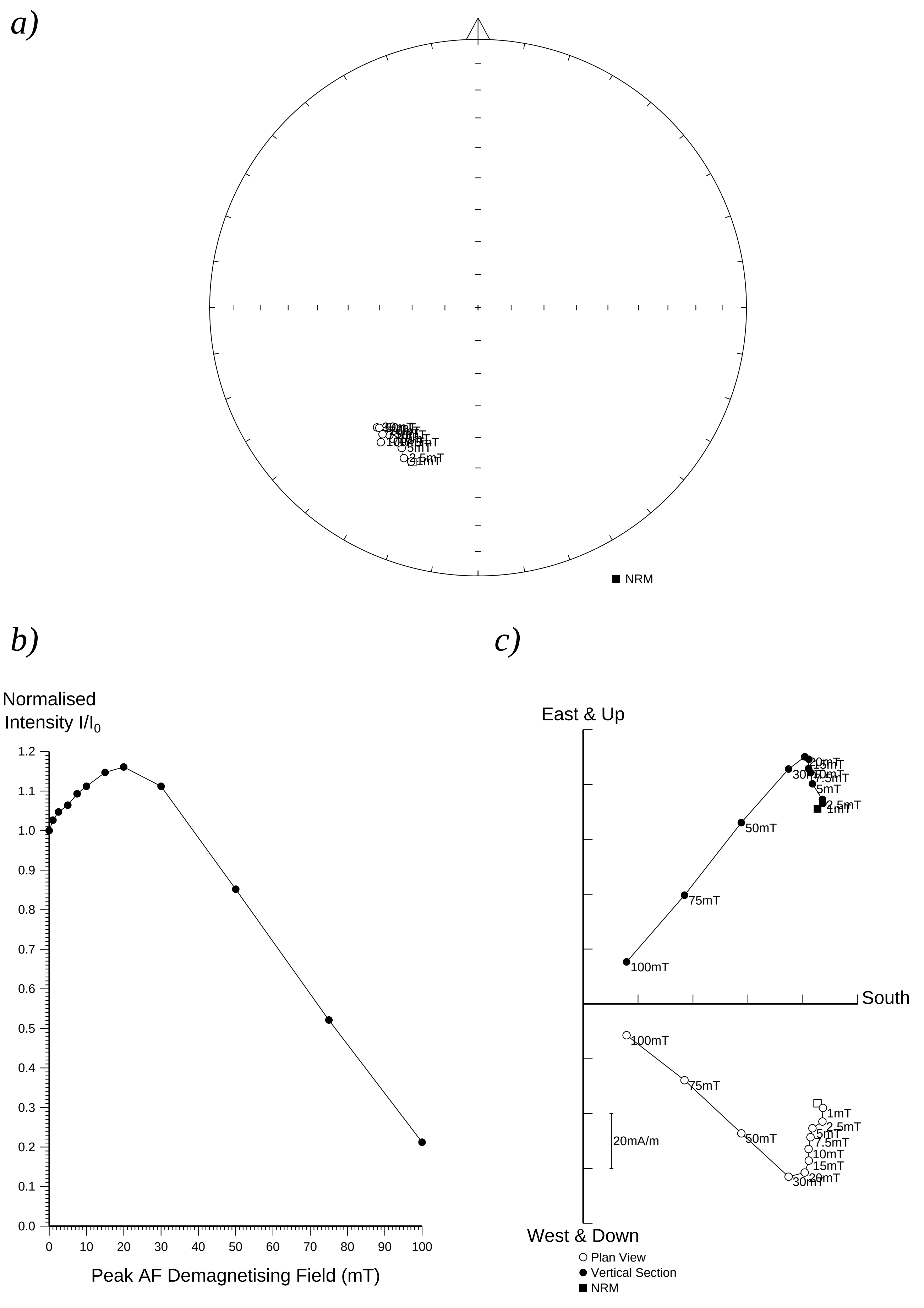

Figure 13: Stepwise AF demagnetisation of sample 2GW12. Diagram a) depicts the variation of the remanent direction as an equal area stereogram (declination increases clockwise, while inclination increases from zero at the equator to 90 degrees at the centre of the projection); b) shows the normalised change in remanence intensity as a function of the demagnetising field; c) shows the changes in both direction and intensity as a vector endpoint projection.

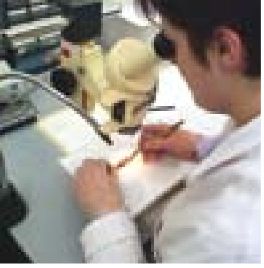
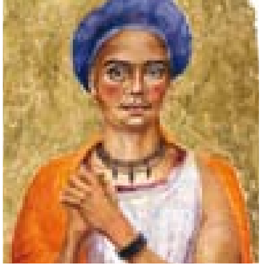



ENGLISH HERITAGE RESEARCH DEPARTMENT

English Heritage undertakes and commissions research into the historic environment, and the issues that affect its condition and survival, in order to provide the understanding necessary for informed policy and decision making, for sustainable management, and to promote the widest access, appreciation and enjoyment of our heritage.

The Research Department provides English Heritage with this capacity in the fields of buildings history, archaeology, and landscape history. It brings together seven teams with complementary investigative and analytical skills to provide integrated research expertise across the range of the historic environment. These are:

* *Aerial Survey and Investigation*
* *Archaeological Projects (excavation)*
* *Archaeological Science*
* *Archaeological Survey and Investigation (landscape analysis)*
* *Architectural Investigation*
* *Imaging, Graphics and Survey (including measured and metric survey, and photography)*
* *Survey of London*

The Research Department undertakes a wide range of investigative and analytical projects, and provides quality assurance and management support for externally-commissioned research. We aim for innovative work of the highest quality which will set agendas and standards for the historic environment sector. In support of this, and to build capacity and promote best practice in the sector, we also publish guidance and provide advice and training. We support outreach and education activities and build these in to our projects and programmes wherever possible.

We make the results of our work available through the Research Department Report Series, and through journal publications and monographs. Our publication Research News, which appears three times a year, aims to keep our partners within and outside English Heritage up-to-date with our projects and activities. A full list of Research Department Reports, with abstracts and information on how to obtain copies, may be found on www.english-heritage.org.uk/researchreports

For further information visit www.english-heritage.org.uk

ENGLISH HERITAGE